

Impact ionization coefficient ratio in InGaAs/InAlAs superlattice avalanche photodiodes determined from noise measurements

Young-June Yu and Gijs Bosman

Department of Electrical Engineering, University of Florida, Gainesville, Florida 32611

P. K. Bhattacharya

Department of Electrical Engineering and Computer Science, University of Michigan, Ann Arbor, Michigan 48109

(Received 22 June 1987; accepted for publication 8 September 1987)

The noise of an $\text{In}_{0.53}\text{Ga}_{0.47}\text{As}/\text{In}_{0.52}\text{Al}_{0.48}\text{As}$ superlattice avalanche photodiode is measured at 700 MHz as a function of applied reverse bias voltage. From the measured data the ratio k of the hole to electron impact ionization coefficients is determined. This ratio is equal to 6 in the field range $(0.8\text{--}2.3) \times 10^5$ V/cm; beyond this range k decreases with increasing field. The field dependence of k is attributed to a transition from ionization across the valence-band-edge discontinuity to band-to-band ionization.

Recently, renewed interest has been given to $p^+i\text{-}n^+$ avalanche photodiodes (APD's) because superlattice i regions are able to enhance the difference between the impact ionization coefficients α and β for electrons and holes, which is an essential requirement for low-noise photodetection.

Since the superlattice APD structures were first proposed,¹ experimental evidence of enhancement of the ionization coefficient ratio has been reported with values of α/β up to 8 for GaAs/AlGaAs APD's.^{2,3} This enhancement of the ionization coefficient ratio is attributed to the fact that the conduction-band discontinuity is larger than the valence-band discontinuity,² and as a result electrons gain more kinetic energy in traversing a heterojunction interface than holes do. Since this sudden gain in kinetic energy increases the probability for impact ionization, α becomes larger than β . More recently, Capasso *et al.*⁴ fabricated $\text{In}_{0.53}\text{Ga}_{0.47}\text{As}/\text{In}_{0.52}\text{Al}_{0.48}\text{As}$ superlattice APD's and reported that $\alpha/\beta \approx 0.05$. This result is surprising since it cannot be explained with the model discussed above. Capasso *et al.* pointed out, however, that for this structure and for the field range considered, the impact ionization of hot carriers with carriers thermally generated and dynamically stored in the quantum wells is responsible for the low field multiplication. This mechanism was first discussed by Smith *et al.*⁵ and later by Chuang and Hess.⁶ Since the valence-band discontinuity ΔE_v is much less than the conduction-band discontinuity ΔE_c at an $\text{In}_{0.53}\text{Ga}_{0.47}\text{As}/\text{In}_{0.52}\text{Al}_{0.48}\text{As}$ interface, the hole confinement is weaker than the electron confinement. As a consequence the holes get released more easily than the electrons from the quantum wells. This mechanism is referred to as "ionization across the band-edge discontinuity."

In our study we used an undoped $\text{In}_{0.53}\text{Ga}_{0.47}\text{As}$ (90 Å)/ $\text{In}_{0.52}\text{Al}_{0.48}\text{As}$ (90 Å) superlattice structure. The impact ionization coefficient ratio presented in this letter was determined from noise experiments for electric field strengths ranging from 0.8×10^5 to 2.7×10^5 V/cm. The experimental data indicate that for a fraction of this range $(0.8\text{--}2.3) \times 10^5$ V/cm, impact ionization across the valence-band-edge discontinuity is responsible for the avalanche multiplication.

As shown in the insert of Fig. 1, our devices are mesa

$p^+i\text{-}n^+$ structures. A 2- μm -thick $n^+\text{-In}_{0.53}\text{Ga}_{0.47}\text{As}$ layer lattice matched to an $n^+\text{-InP}$ substrate was grown, followed by a 1.8- μm -thick undoped $\text{In}_{0.53}\text{Ga}_{0.47}\text{As}/\text{In}_{0.52}\text{Al}_{0.48}\text{As}$ superlattice region consisting of 100 alternating layers and a 2- μm -thick $p^+\text{-In}_{0.53}\text{Ga}_{0.47}\text{As}$ layer for the photoabsorption. For these mole fractions the band-edge discontinuities at the heterojunction interfaces are 0.5 eV for the conduction-band edge and 0.2 eV for the valence-band edge.⁷ The samples were grown using molecular beam epitaxy (MBE). The top layer of the $p^+i\text{-}n^+$ diodes is illuminated by a 1.3- μm InGaAsP light-emitting diode. An optical fiber was used to guide and focus the beam on the APD's. The narrow gap ($E_g = 0.75$ eV) InGaAs material absorbs most of the incoming light, resulting in pure electron injection into the high field superlattice region where multiplication takes place.

Dark current and photocurrent measurements with continuous illumination were performed as a function of reverse bias voltage, and the results are shown in Fig. 1. The

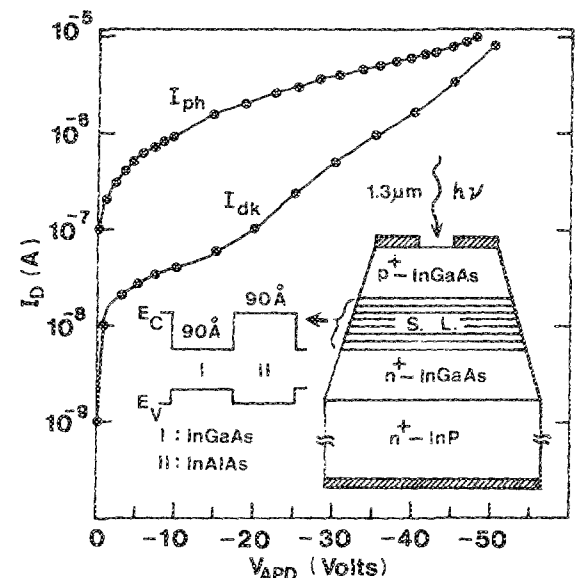


FIG. 1. Dark current and photocurrent characteristics. The insert shows the device configuration and the band diagram of the superlattice structure.

rapid increase in the photocurrent between 0 and 10 V is due to the enhanced collection of photogenerated carriers across the superlattice region with increasing electric field.⁸ Above 15 V the dark current increase is in part due to impact ionization and in part due to the Zener effect taking place in the quantum wells. The device temperature was 300 K during our experiment.

Noise measurements performed between 10 Hz and 25 kHz at room temperature revealed large excess noise levels, probably associated with trapping and detrapping of carriers in quantum wells or traps. These large noise levels result in corner frequencies well above 1 MHz, and a high-frequency, low-noise receiver system had to be designed to measure the noise associated with avalanche multiplication. We combined the advantages of Gasquet's circulator method⁹ and Dicke's modulation technique¹⁰ to build a receiver with a detection limit of 10^{-6} A equivalent noise current and a bandwidth ranging from 500 to 1000 MHz.

Figure 2 shows our experimental setup. The device is mounted on a 50-Ω microstrip line with a 50-Ω termination. By slowly (0.2 Hz) switching between port 1 and port 2 of the microwave switch, the current noise generated in the APD is compared with the reference noise source and averaged for a long time interval. In this way the weak current noise signal which is much smaller than the thermal noise generated in the 50-Ω load resistor can be extracted from the background noise.

In Fig. 3 we present the current noise spectral density measured at 700 MHz versus illuminated diode current. Measurements at other frequencies between 500 and 1000 MHz gave similar results, indicating that the noise is independent of frequency.

A common way to express the current noise S_i of an APD is

$$S_i = 2eI_{pr}M^2F, \quad (1)$$

where M is the multiplication factor defined by the ratio of output current over the primary current and F is called the excess noise factor. The primary current I_{pr} is determined from the breakpoint in Fig. 3 where the slope of S_i vs I_D changes abruptly due to the onset of avalanche multiplication. From Fig. 3 we find $I_{pr} = 1.6 \mu\text{A}$.

In terms of McIntyre's theory¹¹ for band-to-band ionization, F is given by

$$F = M \{1 - (1 - k)[(M - 1)/M]^2\} \quad (2)$$

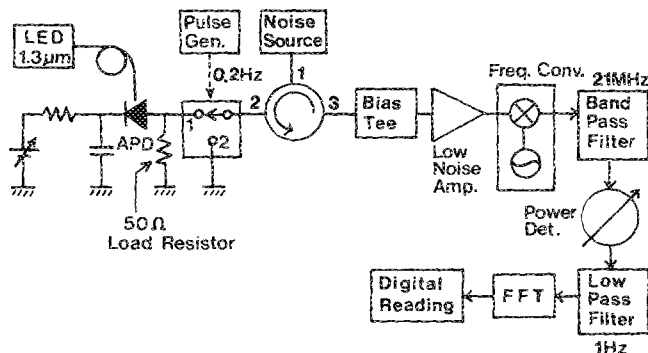


FIG. 2. High-frequency noise measurement setup.

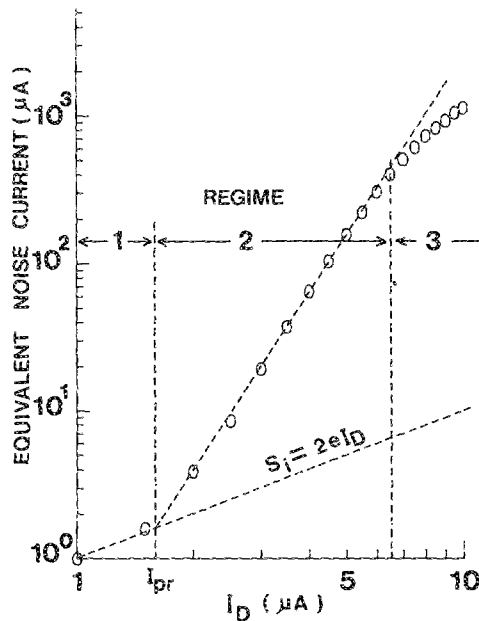


FIG. 3. Measured current noise spectral density vs diode current. Regimes 1, 2, and 3 represent different modes of device operation.

for the case when the primary carriers injected into the avalanche region are electrons. The factor k is equal to β/α . We assume that Eq. (2) also predicts the excess noise caused by ionization across the band-edge discontinuity. In our device, for example, a hole-initiated band-edge ionization triggers the release of a dynamically stored electron from the corresponding quantum well in the conduction band. This release of an electron is required to preserve current continuity. Therefore, ionization across the band-edge discontinuity can be effectively described as a three-particle, band-to-band ionization process and McIntyre's formalism should apply.

In Fig. 4 the experimental values of F as calculated from Eq. (1) are plotted versus the multiplication factor M . Also included are theoretical curves for F calculated using Eq. (2). Note that a breakpoint occurs at $I_D = 6.5 \mu\text{A}$ or $V_{APD} = 41$ V, which corresponds to an electric field of 2.3×10^5 V/cm. Beyond this point the curve of F vs M be-

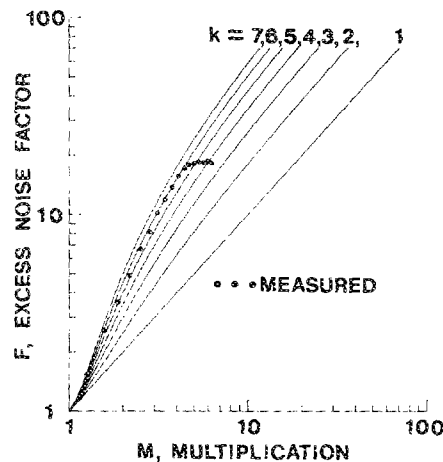


FIG. 4. Excess noise factor vs multiplication. The solid lines indicate theoretical curves for different values of k .¹¹

comes flat and approaches the curve for $k = 1$. This means that the difference between β and α becomes smaller with increasing bias. To explain these results, we introduce three different regimes of operation for this superlattice APD (see Fig. 3).

Regime 1: $0 < V < 15$ V. No multiplication occurs and the noise is equal to full shot noise.

Regime 2: $15 \text{ V} < V < 41$ V. The onset electric field of avalanche multiplication is 8×10^4 V/cm, which is in good agreement with the value reported by Capasso.⁴ This multiplication at low field strengths and the enhancement of β over α are strong indications that impact ionization across the band-edge discontinuity is taking place. Ionization across the band-edge discontinuity is dominant in the valence band because the valence-band discontinuity ($\Delta E_v = 0.2$ eV) is smaller than the conduction-band discontinuity ($\Delta E_c = 0.5$ eV)⁷; consequently, β is larger than α , since it is easier to ionize holes than electrons from the quantum wells.

Regime 3: $41 \text{ V} < V$. Band-to-band ionization sets in, making α and β roughly equal and thereby reducing the value of k . In addition, at these high bias levels the leakage current becomes quite large, mainly due to the Zener effect. This results in mixed current injection into the avalanche region and limits the validity of our discussion, which as-

sumes pure electron injection. Note that the high field breakpoint in the F vs M curve occurs at 2.3×10^5 V/cm, which is very close to the value of 2.5×10^5 V/cm Capasso *et al.* obtained¹² for the onset of band-to-band ionization.

This study was supported by Microfabritech[®] at the University of Florida.

- ¹R. Chin, N. Holonyak, G. E. Stillman, J. Y. Tang, and K. Hess, *Electron. Lett.* **16**, 467 (1980).
- ²F. Capasso, W. T. Tsang, A. L. Hutchinson, and G. F. Williams, *Appl. Phys. Lett.* **40**, 38 (1982).
- ³F. Y. Juang, U. Das, Y. Nashimoto, and P. K. Bhattacharya, *Appl. Phys. Lett.* **47**, 972 (1985).
- ⁴F. Capasso, J. Allam, A. Y. Cho, K. Mohammed, R. J. Malik, A. L. Hutchinson, and D. Sivco, *Appl. Phys. Lett.* **48**, 1294 (1986).
- ⁵J. S. Smith, L. C. Chiu, S. Margalit, A. Yariv, and A. Y. Cho, *J. Vac. Sci. Technol. B* **1**, 376 (1983).
- ⁶S. L. Chuang and K. Hess, *J. Appl. Phys.* **59**, 2885 (1986).
- ⁷R. People, K. W. Wecht, K. Alavi, and A. Y. Cho, *Appl. Phys. Lett.* **43**, 188 (1983).
- ⁸J. Allam, F. Capasso, K. Alavi, and A. Y. Cho, *IEEE Electron Device Lett.* **EDL-8**, 4 (1987).
- ⁹D. Gasquet, J. C. Vassiere, and J. P. Nougier, *Sixth International Conference on Noise in Physical Systems* (NBS Special Publication 614, 1981), p. 305.
- ¹⁰R. H. Dicke, *Rev. Sci. Instrum.* **17**, 268 (1946).
- ¹¹R. J. McIntyre, *IEEE Trans. Electron Devices* **ED-13**, 164 (1966).
- ¹²K. Mohammed, F. Capasso, J. Allam, A. Y. Cho, and A. L. Hutchinson, *Appl. Phys. Lett.* **47**, 597 (1985).